Room temperature direct-bandgap electroluminescence from a horizontal Ge ridge waveguide on Si*

Chao He(何超), Zhi Liu(刘智), and Bu-Wen Cheng(成步文)†

State Key Laboratory on Integrated Optoelectronics, Institute of Semiconductors, Chinese Academy of Sciences, Beijing 100083, *China*

(Received 15 June 2016; revised manuscript received 21 August 2016; published online 25 October 2016)

We report a lateral Ge-on-Si ridge waveguide light emitting diode (LED) grown by ultrahigh vacuum chemical vapor deposition (UHV-CVD). Direct-bandgap electroluminescence (EL) of Ge waveguide under continuous current is observed at room temperature. The heat-enhancing luminescence and thermal radiation-induced superlinear increase of edge output optical power are found. The spontaneous emission and thermal radiation based on the generalized Planck radiation law are calculated and fit very well to the experimental results. The Ge waveguides with different lengths are studied and the shorter one shows stronger EL intensity.

Keywords: Ge/Si, waveguide, electroluminescence, thermal radiation

PACS: 61.72.uf, 42.79.Gn, 78.60.Fi, 44.40.+a **DOI:** 10.1088/1674-1056/25/12/126104

1. Introduction

An efficient and reliable Si-based light source is an extremely key component of optoelectronic integrated circuit (OEIC). In order to achieve this goal, unremitting efforts have been made in the past years.[1–3] Ge-on-Si has emerged as a promising candidate because of its high compatibility with the conventional Si complementary metal–oxide–semiconductor (CMOS) process, and its pseudo direct bandgap structure.[4] Quantum confinement effect[5] and strain engineering are the common methods used to improve the luminous efficiency of Ge. According to the deformation potential theory,[6] the band offset between direct bandgap and indirect bandgap of Ge can be reduced by tensile strain. Under adequate strain and n-type doping, population inversion can be obtained in the direct bandgap of Ge. Much progress has been made in recent years in the photoluminescence (PL) and electroluminescence (EL) of direct bandgap transition of Ge on Si substrate.[7–10] In particular the breakthrough results of Ge direct bandgap lasing by optical pumping[11] and electrical pumping[12,13] further confirmed the validity of the theoretical framework.

In an optical pumping laser, the main optical losses are the facet loss and free carrier absorption loss. The theoretical facet loss is only 2 cm^{-1} for a perfect mirror.[11] Vertical Si/Ge/Si or Ge/Ge/Si structure is most commonly used in electrical pumping laser in the above references. In these cases, additional losses of more than 100 cm^{-1} induced by the electrode and high-doped injecting layer on the top of Ge waveguide must be overcome.[12] Based on the consideration of monolithic integration and reducing additional losses, we previously proposed a lateral PIN ridge waveguide structure on Si.[14] The electrical contacts were designed on the two sides of the Ge waveguide and far away from the waveguide to reduce metal absorption loss. No more cap layer like poly-Si was needed. In this work, we optimize this structure for improving the luminous efficiency. The Ge waveguide is n-type doped with phosphorus and a shorter waveguide is cleaved to provide better optical feedback. Experimental results show that the device has good performances of light confinement and excellent carrier-injecting efficiency.

2. Material growth and device fabrication

The Ge film was grown on high-resistance Si (001) substrate with a resistivity of about 5000 Ω·cm by UHV-CVD. The Ge film was *in situ* doped with phosphorus and 850 nm in thickness determined by scanning electron microscope (SEM). To improve the lattice quality and tensile strain, the Ge film was deposited with 300-nm SiO_2 grown by plasma enhancement chemical vapor deposition (PECVD), and then rapid thermal annealed (RTA) *ex situ* at 900 °C for 15 s in nitrogen atmosphere. As a result, an in-plain tensile strain about 0.2% was introduced into the Ge film, determined by x-ray diffraction and Raman spectrum.[15] The effective n-type doping level was about 1×10^{18} cm^{-3} measured by Hall effect. Afterwards, the Ge film capped with SiO_2 was patterned into ridge waveguide structures along the (110) direction. The two sides of the Ge ridge were subsequently implanted with phosphorous and boron ions up to a doping level of 10^{20} cm^{-3} measured by secondary ion mass spectrometry (SIMS). After dopant activation annealed at 600 °C, 600-nm SiO_2 was deposited by PECVD and the contact holes were formed by

*Project supported by the National Basic Research Program of China (Grant No. 2013CB632103), the National Natural Science Foundation of China (Grant Nos. 61176013 and 61036003), and the Science Fund from Beijing Science and Technology Commission, China (Grant No. Z151100003315019).

†Corresponding author. E-mail: cbw@semi.ac.cn

© 2016 Chinese Physical Society and IOP Publishing Ltd

dry etching. A metal stack consisting of Ni/Al/Ti/Au was deposited as the electrodes and thermally activated at 400 °C to form good ohmic contact. The thickness of the samples remained about 100 μm after mechanical polishing. Ge ridge waveguides with different lengths were cleaved to expose the (110) facets as the Fabry–Perot mirrors to provide optical feedback in the edge emitter. The schematic diagram of the device of the Ge ridge waveguide LED is shown in Fig. 1(a).

3. Results and discussion

The current–voltage (I–V) characteristics of the Ge-on-Si ridge waveguide LED were measured by an Agilent B1500A semiconductor device analyzer. The I–V curve of the device is shown in Figure 1(b). The device exhibits a well-defined rectifying behavior with a dark current density of about 2 A/cm^2 at 1-V reverse bias. The ideality factor η for p–n junction can be estimated using the empirical formula:[16]

$$J \propto \exp\left[(qV)/(\eta k_{\mathrm{B}} T)\right], \tag{1}$$

where J is the current density, V the voltage, q the elementary charge, k_{B} the Boltzmann constant, and T the absolute temperature.

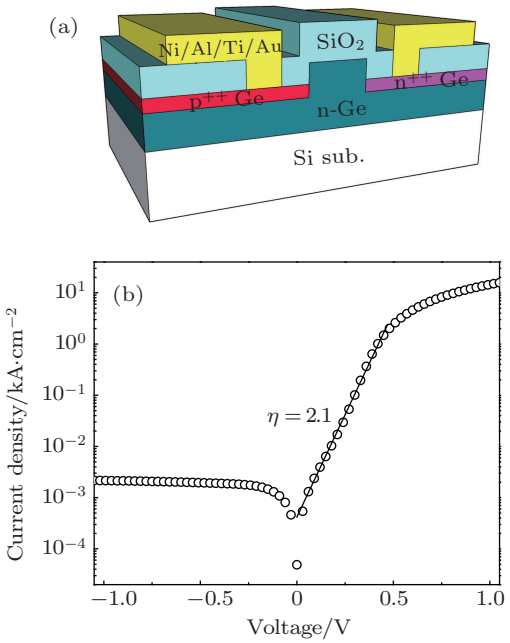


Fig. 1. (color online) (a) (color online) Schematic diagram of the Ge-on-Si ridge waveguide LED. (b) The I–V characteristic of the Ge-on-Si ridge waveguide LED.

In our case, while voltage is less than 0.45 V, the η is about 2.1, which is very close to 2 for an ideal PIN junction.[16] This means that our device has an excellent carrier-injecting efficiency. When voltage is larger than 0.45 V, η increases because of the large carrier injection effect and the series resistance effect. Compared with the vertical heterostructure PN junction, the injected carriers in our lateral PIN junction would not transport across the Ge/Si hetero-interface where large numbers of dislocations exist. This would effectively avoid non-radiative recombination caused by defects at the interface.

The EL characteristics of the Ge-on-Si ridge waveguide LED were measured by a LabRam HR800 Raman Instrumentation with an InGaAs photodetector at room temperature. The edge EL spectra under different currents are shown in Fig. 2(a). The wavelength of the EL peak is located near 1580 nm due to the detection wavelength limit of our InGaAs photodetector, resulting in an uncompleted EL spectrum. The actual peak position is expected at approximately 1610 nm when considering the 0.2% thermal tensile strain.

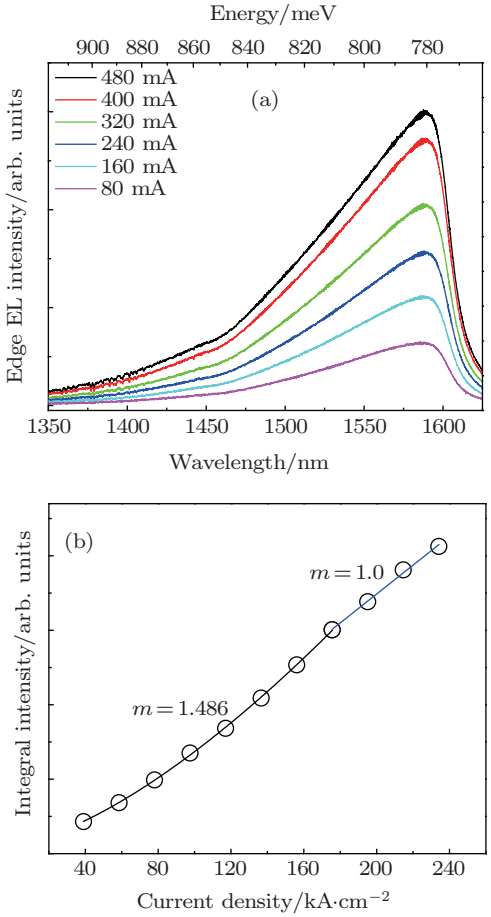


Fig. 2. (color online) (a) Direct-bandgap EL spectra of edge emission under different currents. The length of Ge waveguide is 270 μm. (b) Relationship between integral EL intensity and current density, which is characterized by $L \propto J^m$.

Figure 2(b) shows the current dependence of integral EL intensity. The dependence is characterized empirically by the relation $L \propto J^m$, where L refers to the integral EL intensity and J is current density. The extracted exponent m is 1.486 when current density is less than 175 kA/cm^2. This superlinear effect is mainly caused by the increasing device temperature by Joule heating.[10] But the EL intensity shows almost linear dependence on large current density, which is probably caused by the spectrometer detection limit.

Figure 3 shows the edge optical output power of the Ge-on-Si ridge waveguide LED under continuous current and the

fitted curve with thermal radiation and spontaneous emission. The output optical power is measured by coupling the Ge waveguide with a commercial InGaAs detector. As the inset shows in the figure, the output power of the Ge waveguide increases superlinearly in a small current range, and the exponent of output power is 1.487, which is extremely close to that of integral EL intensity. While the current density is larger than 230 kA/cm^2, the output power of the Ge waveguide increases dramatically.

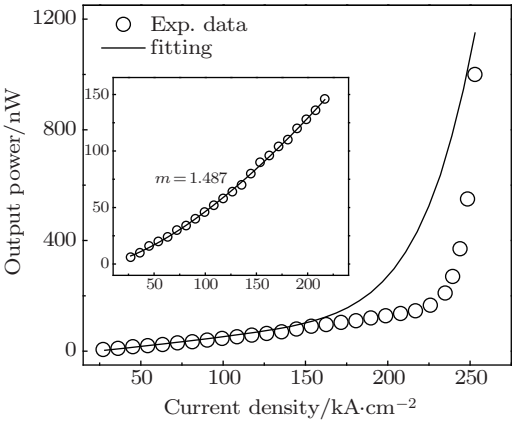


Fig. 3. Optical output power pumped by continuous current and the fitted results. The inset shows the relationship before the onset of dramatic increase.

We attribute this lasing-similar phenomenon when $J >$ 230 kA/cm^2 to thermal radiation of Ge. It is found that when the injection current reaches threshold, the electrode of the device tends to be melted and disconnected. The melting point of Al is 660 °C, which is the minimum melting point of our metal stack. In this high-temperature range, the thermal emission of the membranes could not be ignored.[17] The emitted radiation per photon energy interval is proportional to

$$R(E) \propto \frac{\alpha(E)E^3}{\exp\left(\dfrac{E-\mu}{k_{\mathrm{B}}T}\right)-1}, \tag{2}$$

where E is the photon energy, μ the chemical potential, and α the absorption coefficient. The chemical potential $\mu = 0$ for thermal radiation and $\mu = E_{\mathrm{fe}} - E_{\mathrm{fh}}$ for luminescence where E_{fe} and E_{fh} is the quasi-Fermi energy for electron and hole, respectively. For the direct band gap recombination of Ge, the absorption can be described as

$$\alpha = A\sqrt{E-E_{\mathrm{g}}}\left[f_{\mathrm{v}}(E_{\mathrm{v}}) - f_{\mathrm{c}}(E_{\mathrm{c}})\right], \tag{3}$$

where A is constant, E_{g} the direct bandgap of Ge, f_{c} and f_{v} the Fermi–Dirac distribution functions of electron and hole, E_{c} and E_{v} the energy levels of electron and hole, respectively.[18] As the corresponding device temperature of current density is hard to reliably determine, the temperature from room temperature to the melting point of Al is set to linearly depend on current density for simplicity. Thus the spontaneous emission and thermal radiation power are calculated and used to fit the experimental data. The result is shown in Fig. 3. We note that according to our calculation, the spontaneous emission power almost linearly increases with temperature rising, which agrees with the published results, while the thermal radiation power superlinearly increases with temperature rising.

To study the EL distribution of the Ge waveguide, we investigate the emission properties of different surface positions of Ge ridge waveguide as shown in Fig. 4(a). The P and N regions refer to the boron and phosphorus ion-implanted regions next to the Ge ridge waveguide, while WG refers to the top surface of the waveguide. As depicted in the figure, the EL intensity from the Ge waveguide is larger than those from P and N regions. It means that the light is mainly constricted in the waveguide. This is easy to understand because most direct-bandgap radiative recombination of the carriers happens here. It is worth noting that the EL intensity in N region is stronger than that in P region. Actually, a small part of the carriers recombine radiatively on the two sides of the waveguide. As a pseudo-direct bandgap, Ge emission intensity is nearly proportional to the electron concentration in Γ valley. The electron concentration of Γ valley in N region is larger than that in P region, resulting in stronger EL intensity.

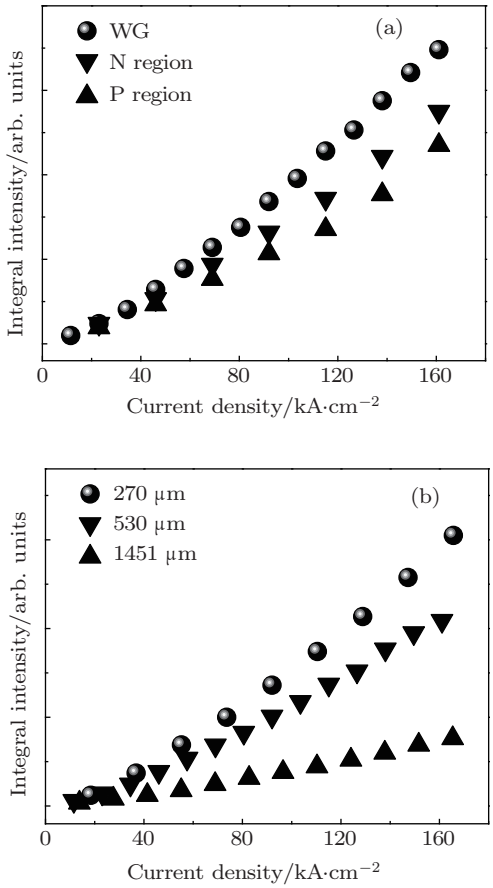


Fig. 4. Integral EL intensities (a) at different surface positions and (b) of different length of Ge-on-Si ridge waveguide. The width of the waveguide is about 1.2 μm.

The emission properties of different lengths of Ge waveguide are investigated. As shown in Fig. 4(b), the integral EL

intensity increases as the length of waveguide reduces. A possible reason, we think, is that below the optical gain, Ge is an absorbing medium other than a gain one. Therefore, the light is absorbed more in a longer waveguide.[19]

4. Conclusions

In this paper, a lateral injection Ge ridge waveguide structure is proposed, which possesses the merits of simple manufacturing process, high injection efficiency, and low optical loss. A Ge ridge waveguide LED is fabricated by implementing a CMOS-compatible technology, and the direct-bandgap EL under continuous current is observed at room temperature. Different positions of the Ge ridge waveguide are measured and the waveguide shows good performances of light confinement. The heat-enhancing luminescence and thermal radiation-induced superlinear increase of output optical power are found. This lasing-like phenomenon is explained by the model of generalized Planck law and fitted well to the experimental results.

References

[1] Tanabe K, Watanabe K and Arakawa Y 2012 *Sci. Rep.* **2** 349

[2] Wirths S, Geiger R, von den Driesch N, Mussler R, Stoica T, Mantl S, Ikonic Z, Luysberg M, Chiussi S, Hartmann J M, Sigg H, Faist J, Buca D and Grützmacher D 2015 *Nat. Photon.* **9** 88

[3] Chen S, Li W, Wu J, Jiang Q, Tang M, Shutts S, Elliott S N, Sobiesierski A, Seeds A J, Ross I, Smowton P M and Liu H 2016 *Nat. Photon.* **10** 307

[4] Liu J, Sun X, Pan D, Wang X, Kimerling L C, Koch T L and Michel J 2007 *Opt. Express* **15** 11272

[5] Samavati A, Othaman Z, Ghoshal S K and Mustafa M K 2015 *Chin. Phys. B* **24** 028103

[6] Liu J, Cannon D D, Wada K, Ishikawa Y, Danielson D T, Jongthammanurak S, Michel J and Kimerling L C 2004 *Phys. Rev. B* **70** 155309

[7] Sun X, Liu J, Kimerling L C and Michel J 2009 *Appl. Phys. Lett.* **95** 011911

[8] Hu W, Cheng B, Xue C, Xue H, Su S, Bai A, Luo L, Yu Y and Wang Q 2009 *Appl. Phys. Lett.* **95** 092102

[9] Sun X, Liu J, Kimerling L C and Michel J 2009 *Opt. Lett.* **34** 1198

[10] Cheng S L, Lu J, Shambat G, Yu H Y, Saraswat K, Vuckovic J and Nishi Y 2009 *Opt. Express* **17** 10019

[11] Liu J, Sun X, Camacho-Aguilera R, Kimerling L C and Michel J 2010 *Opt. Lett.* **35** 679

[12] Camacho-Aguilera R E, Cai Y, Patel N, Bessette J T, Romagnoli M, Kimerling L C and Michel J 2012 *Opt. Express* **20** 11316

[13] Koerner R, Oehme M, Gollhofer M, Schmid M, Kostecki K, Bechler S, Widmann D, Kasper E and Schulze J 2015 *Opt. Express* **23** 14815

[14] Liu Z, Li Y, He C, Li C, Xue C, Zuo Y, Cheng B and Wang Q 2014 *Appl. Phys. Lett.* **104** 191111

[15] Liu Z, Cheng B W, Li Y M, Li C B, Xue C L and Wang Q M 2013 *Chin. Phys. B* **22** 116804

[16] Sze S M and Ng K K 2006 *Physics of semiconductor devices* (New York: John Wiley & Sons) p. 98

[17] Boucaud P, Kurdi M E, Sauvage S, de Kersauson M, Ghrib A and Checoury X 2013 *Nat. Photon.* **7** 162

[18] Coldren L A, Corzine S W and Mashanovitch M L 2012 *Diode lasers and photonic integrated circuits* (New York: John Wiley & Sons) p. 172

[19] Okumura T, Oda K, Kasai J, Sagawa M and Suwa Y 2016 *Opt. Express* **24** 9132